Accepted Manuscript

Effects of *in utero* androgen excess and metformin treatment on hepatic functions

Giselle Adriana Abruzzese, María Florencia Heber, María José Ferrer, Silvana Rocío Ferreira, Aimé Florencia Silva, Alicia Beatriz Motta

PII: S0303-7207(19)30082-6

DOI: https://doi.org/10.1016/j.mce.2019.03.006

Reference: MCE 10416

To appear in: *Molecular and Cellular Endocrinology*

Received Date: 12 September 2018

Revised Date: 8 March 2019

Accepted Date: 8 March 2019

Please cite this article as: Abruzzese, G.A., Heber, Marí.Florencia., Ferrer, Marí.José., Ferreira, Silvana.Rocí., Silva, Aimé.Florencia., Motta, A.B., Effects of *in utero* androgen excess and metformin treatment on hepatic functions, *Molecular and Cellular Endocrinology* (2019), doi: https://doi.org/10.1016/j.mce.2019.03.006.

Effects of *in utero* androgen excess and metformin treatment on hepatic functions

Giselle Adriana Abruzzese [a*], María Florencia Heber [a*], María José Ferrer [a], Silvana Rocío Ferreira [a], Aimé Florencia Silva [a], Alicia Beatriz Motta PhD [a].

[a] Laboratorio de Fisio-patología Ovárica, Centro de Estudios Farmacológicos y Botánicos (CEFYBO), Consejo Nacional de Investigaciones Científicas y Tecnológicas (CONICET), Facultad de Medicina, Universidad de Buenos Aires (UBA), Paraguay 2155, CP1121, Ciudad Autónoma de Buenos Aires, Argentina.

[*] These authors contributed equally to this study.

***Corresponding author:** ABM; aliciabmotta@yahoo.com.ar; CEFYBO-UBA-CONICET, Facultad de Medicina, Universidad de Buenos Aires (UBA), Paraguay 2155, 17th floor, CP1121, Ciudad Autónoma de Buenos Aires, Argentina.

Abstract

This study aimed to evaluate the role of prenatal hyperandrogenization in liver functions and the extent of metformin as treatment. Pregnant rats were hyperandrogenized with subcutaneous testosterone (1mg/rat) between 16 and 19 of pregnancy. Prenatally hyperandrogenized (PH) female offspring displayed, at the adult life, two phenotypes; a PH irregular ovulatory phenotype (PHiov) and a PH anovulatory (PHanov) phenotype. From day 70 to the moment of sacrifice (90 days of age), 50% of the animals of each group received a daily oral dose of 50 mg/kg of metformin. We found that both PH phenotypes displayed a hepatic disruptions of insulin and glucose pathway and that metformin treatment reversed some of these alterations in a specific-phenotype manner. Our findings show, for the first time, that androgen excess *in utero* promotes hepatic dysfunctions and that metformin treatment is able to specifically reverse those hepatic alterations and sheds light on the possible mechanisms of metformin action.

Key words: Fetal programming; PCOS; liver; insulin pathway; metformin.

1. Introduction

The liver is the organ that controls body energy metabolism. It is responsible for glucose and insulin metabolism, energy storage and lipid availability (Paschos and Paletas, 2009). Thus, alterations in these pathways may lead to the development not only of liver diseases but also of metabolic disorders (Paschos and Paletas, 2009; Vassilatou, 2014). It is known that androgens contribute to hepatic dysfunctions; however the exact mechanism remains unknown. Some studies have reported a close

relationship between an increased androgen bioavailability and the development of hepatic alterations in patients with a hyperandrogenemic condition such as polycystic ovary syndrome (PCOS) (Vassilatou, 2014; Vassilatou et al., 2010).

Increasing evidence suggests that the *in utero* exposure of fetuses to certain hormonal, nutritional, metabolic, and environmental factors is able to induce permanent health disorders in the offspring. It has been reported that maternal androgen excess in rats, alters placental steroidogenesis and leads to dysregulation of lipid metabolism in their adult female offspring (Sun et al., 2012). Likewise, prenatal androgen excess affects fetal liver function with increased triglyceride content and alters expression of enzymes and transcription factors involved in *de novo* lipogenesis and fat storage (Fornes et al., 2017). In this context, we have previously demonstrated that prenatal hyperandrogenism induces liver alterations and impairs the balances of both lipid metabolism and systemic insulin and glucose metabolism (Abruzzese et al., 2016). We have also found deeper alterations in the anovulatory phenotype than in the ovulatory phenotype . These data led us to hypothesize that prenatal androgen excess could lead to alterations in glucose and insulin metabolism and thus, altering liver function during the adult life.

The biguanide metformin is currently the most used insulin sensitizer in the treatment of insulin resistance in type 2 diabetes, gestational diabetes and PCOS, but is also effective in the treatment of other pathologies such as different types of cancers and non-alcoholic liver disease . One of the most important properties of metformin is its pleiotropic actions on tissues affected by insulin resistance and/or hyperinsulinemia (Diamanti-Kandarakis et al., 2010; Legro et al., 1999). It is known that the effect of metformin on the inhibition of hepatic gluconeogenesis involves several cascades. The proposed mechanisms range from a direct inhibition of gluconeogenic enzymes and a reduced hepatic uptake of substrates of gluconeogenesis to mechanisms involving insulin signaling such as insulin receptor substrates (IRS)-1 and -2 (Corbould and Dunaif, 2007). It has also been demonstrated that metformin may reduce the supply of energy required for gluconeogenesis by inhibition of mitochondrial respiration (De Fea and Roth, 1997) and stimulate glucose entry into the liver and glycolysis (Book and Dunaif, 1999). However, the complete mechanism by which metformin is able to increase insulin sensitivity remains unknown. Based on the above observations, the aim of the present work was to study the long-term effects of prenatal androgen excess on the hepatic glucose and insulin pathways. We were also interested in revealing the possible role of metformin treatment in restoring these possible alterations caused by

fetal programming.

2. Materials and methods

2.1. Animals and experimental design

Virgin female rats of the Sprague Dawley strain mated with fertile males of the same strain were used. Three females and one male were housed in each cage under controlled conditions of light (12 h light, 12 h dark) and temperature (23-25 ºC). Animals received food and water *ad libitum*. Day 1 of pregnancy was defined as the morning in which spermatozoa were observed in the vaginal fluid. Between days 16 and 19 of pregnancy, rats were hyperandrogenized as described previously (Abruzzese et al., 2016; Demissie et al., 2008). Briefly, a group of pregnant rats (N = 15) received daily subcutaneous (SC) injections of 1 mg of free testosterone (T-1500; Sigma) dissolved in 100 µl of sesame oil (vehicle) between 16 and 19 of pregnancy. The dose of testosterone administered resulted in circulating testosterone levels similar to those of male rats (Wolf et al., 2002). A second group (N = 10) was SC injected with 100 µl of vehicle only. Under the conditions of our animal facilities, spontaneous term labor occurs on day 22 of gestation. Pups were culled from litters to equalize group sizes (10 pups per mother). Female offspring were separated from males at 21 days of age and randomly chosen. The offspring (N=60) from hyperandrogenized mothers formed the prenatally hyperandrogenized (PH) group and the offspring (N=30) from mothers that received vehicle only formed the control group. Animals were allowed free access to Purina rat chow (Cooperación, Argentina) and water. All the procedures involving animals were conducted in accordance with the Animal Care and Use Committee of Consejo Nacional de Investigaciones Científicas y Técnicas, Argentina, and the study was approved by the Ethics Committee of the School of Medicine of the University of Buenos Aires, Argentina. The estrous cycle was determined by vaginal smears taken daily from 45 to 70 days of age. The PH group showed two phenotypes: *i) Anovulatory phenotype* (PHanov): animals whose smears showed metaestrus, diestrus, or a combination of both for four consecutive days, and were thus considered to be non-cycling; ii*) Irregular ovulatory phenotype* (PHiov): animals that showed some smears displaying the four stages of the estrous cycle: proestrus, estrus, metaestrus, and diestrus with cycles of 7 days or longer (Abruzzese et al., 2016). Animals from the control, PHiov and PHanov groups showed no significant differences in body weight (231±15, 238±22 and 231±19 g, respectively). Serum testosterone levels, determined by radioimmunoassay (RIA)

(Amalfi et al., 2012), were increased in both PH phenotypes, being higher in the PHanov group than in the PHiov and control groups (control= 67.76 ± 13.52; PHiov= 115.84 ± 34.82; PHanov= 154.34 ± 32.00; control + Metformin= 101.27 ± 17.35; PHiov= 123.73 ± 35.90; PHanov= 129.34 ± 10.65). As it has been previously reported (Heber et al., 2019), metformin treatment did not modify the testosterone levels of the PHiov or PHanov groups, but tended to diminish those of the PHanov group.

From day 70 to the moment of sacrifice, day 90 of age, 50% of the animals of each group received a daily oral, by a tip each one, dose of 50 mg/kg of metformin (Fig. 1).

The dose of metformin used for the study was the maximum dose daily used in the treatment of women with PCOS (Lashen, 2010).

As the PHanov group remained in diestrus, to allow the comparison between the phenotypes, all animals were euthanized at this stage. Then, on the first diestrus at 90 days of age, the female offspring from each group were weighed, anesthetized with carbon dioxide and killed by decapitation. Trunk blood was collected and serum was separated and kept at -80°C for further studies. The liver were separated and conserved at -80°C. All animals were randomly assigned to each assay considering the littermate. Thus, each assay was carried out with the same number of PHiov and PHanov animals from each randomly selected littermate.

2.2 Serum glucose and insulin levels and HOMA-IR determination

Fasting (for 8h) blood glucose was determined by using Accu-Chek test strips (Roche) for visual determination in the range of 20–800 mg/100 ml (1–44 mmol/l) (N=10 per group), the accuracy of the system is the 97% as comparing with the biochemical assay as informed by the manufacturer's instructions. Fasting (for 8h) insulin levels were measured by an ELISA kit, following the manufacturer's instructions (Abcam Insulin Human ELISA Kit: Insulin human ELISA kit ab 100578 but that reacts with: mouse, rat, human and pig. The sensitity is < 4 µIU/ml and the range 4,69 µIU/ml - 300 µIU/ml). Serum glucose levels were expressed as mg/dl and insulin levels as µIU/ml. The homeostatic model assessment for insulin resistance (HOMA-IR) was calculated according to the formula: fasting insulin (µIU/ml) x fasting glucose (mg/dl)/405 (Matthews et al., 1985).

2.3 Gene expression of insulin receptor (IR), IRS1, IRS2, Pepck-1, glucose transporter Glut2, Chrebp, Srebp and Pparg

The mRNA levels of *IR, IRS1, IRS2, Pepck, Glut 2, Chrebp, Srebp and Pparg* were measured by Real-Time polymerase chain reaction (Real-Time PCR) analysis. Total

mRNA from hepatic tissue (6 samples per group, per tissue) was extracted by using RNAzol RT (MRC gene, Molecular Research Center, OH, USA), following the manufacturer's instructions. cDNA was synthesized from 500 ng mRNA by using random primers. Real-Time PCR analysis was performed from this cDNA by means of the real mix B124-100 (Biodynamics SRL, USA). The amplified products were quantified by fluorescence, using the Rotor Gene 6000 Corbette. Results are expressed as arbitrary units. The 60s Ribosomal protein L32 (RPL32) and Proteasome subunit beta type-2 (PSMB2) were used as reference genes.

Gene expression was quantified using the comparative CT method (also known as the $2^{-\Delta\Delta CT}$ method) (Swillens et al., 2008). Primers are shown in Table 1. Results are expressed as arbitrary expression of mRNA referred to L32 and PSMB2.

2.4 Energy storage and hepatic alterations

2.4.1 Hepatic glycogen content

Hepatic glycogen content was measured by the method of Seifter and Dayton (Seifter and Dayton, 1950). Briefly, hepatic tissue was digested in boiling KOH and then glycogen was precipitated in ethylic alcohol and dissolved in water, and heated together with anthrone reagent. This procedure converts glycogen into glucose. The developed green product was read at 620nm. The amount of glycogen obtained was expressed as mg glycogen/100 mg hepatic tissue.

2.4.2 Hepatic triglyceride content

To evaluate the triglyceride (TG) content in the liver, 10 frozen samples of each group were saponified and the TG content quantified by comparing with a glycerol standard curve by using a commercial kit (Wiener Lab, Argentina), as described previously (Chow et al., 2011). Results are expressed as mg/g tissue.

2.4.3 Hepatic enzymes

Serum levels of alanine aminotransferase (ALT), aspartate aminotransferase (AST) and gamma-glutamyl transferase (GGT) were quantified by colorimetric enzymatic methods (Wiener Lab, Argentina) as previously reported (Abruzzese et al., 2016) and following the manufacturer´s instructions. The chromophoric products were measured at 340 nm for ALT and AST and at 405 nm for GGT, all at 25 °C. The values of the intra- and interassay coefficients of variation were 3.02 and 5.63% for ALT, 4.4 and 4.9% for AST and 1.62 and 5.0% for GGT. Results are expressed as IU/l.

Liver oxidant/antioxidant balance

The oxidant-antioxidant balance in liver tissue was evaluated as the lipid peroxidation index and the content of the antioxidant glutathione (GSH) in 10 samples from each group. The results are expressed as TBARs nM/g tissue for the lipid peroxidation index and as µM/g tissue for GSH.

Circulating lipid profile

To determine the systemic lipid profile, total cholesterol, high density lipoprotein (HDL), and triglycerides were quantified by colorimetric-enzymatic methods (Weiner Lab). The chromophoric product was measured at 505 nm for cholesterol, at 600 nm for HDL, and at 490 nm for triglycerides. Low density protein (LDL) cholesterol was estimated indirectly by the following formula: LDL= Total cholesterol - HDL + Triglycerides/5 (Friedewald et al., 1972).

Mechanism of metformin action

It is known that metformin acts through the activation of AMPK. In order to determine its activation, we evaluated the protein expression of the substrate of activated AMPK, the phosphorylated acetyl CoA carboxylase (pACC) (Lee et al., 2018). By Western Blot analysis we evaluated the hepatic protein expression of pACC in control and PH phenotypes. Briefly, Western blotting was performed as previously described (Amalfi et al., 2012). Liver tissue (n= 7 per group) was lysed for 20 min at 4 ºC in lysis buffer (20 mM Tris-HCl, pH= 8.0, 137 mM NaCl, 1% Nonidet P-40 and 10% glycerol) supplemented with protease inhibitors (Protease Inhibitor Cocktail P8340, Sigma Aldrich, St. Louis MO, USA). The lysate was centrifuged at 4 ºC for 10 min at 10,000g and the pellet discarded. Protein concentrations in the supernatant were measured by the Bradford assay (Bio-Rad) (Bradford, 1976). Total proteins (50 µg) were denatured and separated on a SDS-polyacrylamide gel (10%) and transferred onto nitrocellulose membranes (GE Healthcare, Life Sciences). Membranes were blocked for 1.5 h in TBS (4 mM Tris-HCl, pH= 7.5, 100 mM NaCl) containing bovine serum albumin (5%) at room temperature, and, subsequently, the membranes were washed three times for 7 min each in TBST (4 mM Tris-HCl, pH= 7.5, 100 mM NaCl, 0.1% Tween 20) and then incubated at 4°C with rocking overnight with the primary antibody; Phopho-Acetyl-CoA Carboxylase (Ser79) Antibody (#3661 Cell Signalling), in a 1:2000 dilution. Then, the membranes were washed three times for 7 min each in TBST and incubated at room temperature for 1 h with peroxidase-conjugated species-specific antirabbit and antimouse IgG while being rocked. Then, after three washings of 7 min each with TBST, the bound antibodies were detected with an enhanced chemiluminescence

system, ImageQuant LAS 500 (GE Healthcare, Life Sciences). Band intensities were quantified by scanning densitometry by using Image J 1.44p software (Wayne Rasband, NIH, USA) and normalized relative to B-tubulin and expressed as arbitrary units (AU).

3. Statistical analysis

Statistical analyses were carried out using the program GraphPad Instat® (GraphPad software, San Diego, CA, USA). Two-way ANOVA with post-hoc Bonferroni test was used to compare the six groups (Control, PHiov and PHanov without metformin treatment and Control, PHiov and PHanov with metformin treatment). Statistical significance was considered as $p< 0.05$.

4. Results

4.1 Effects of prenatal hyperandrogenization on circulating insulin resistance

Regarding the effect of prenatal hyperandrogenization on circulating insulin resistance, we evaluated serum glucose and insulin levels and the HOMA-IR index.

Prenatal hyperandrogenization led to an increase in the basal glucose serum levels of both the PHiov and PHanov phenotypes (Fig. 2A). Metformin treatment was able to reverse this adverse effect in both PH phenotypes (Fig. 2A; a vs. b $p<0.01$).

Prenatal hyperandrogenization also led to an increase in the basal insulin serum levels of both phenotypes (Fig. 2B). Metformin treatment partially reversed this effect in the PHanov phenotype. The PHiov showed a tendency to be normalized to control values but this tendency was not statistically significant (Fig. 2B; a vs. b, $p<0.01$).

Prenatal hyperandrogenization also led to an increase in HOMA-IR ($p<0.01$) in both PH phenotypes (Fig. 2C). Metformin was able to reverse this adverse effect in both phenotypes (Fig. 2C).

4.2 Effect of prenatal hyperandrogenization on disrupting of hepatic insulin signaling

To establish the impact of prenatal hyperandrogenization on hepatic insulin signaling disruption we evaluated the gene expression of the first molecules involved in the insulin receptor pathway: *IR*, *IRS1* and *IRS2*. Prenatal hyperandrogenization decreased ($p<0.01$) the gene expression of *IR* from liver tissue from both PH phenotypes and metformin treatment was not able to reverse this effect (Fig. 3A). Prenatal hyperandrogenization also decreased ($p<0.01$) the gene expression of *IRS1* from liver tissue from both phenotypes, and metformin reversed this decrease leading the gene expression of *IRS1* to control values (Fig. 3B, $p<0.01$).

Prenatal hyperandrogenization also decreased ($p<0.01$) the gene expression of *IRS2* from both phenotypes and metformin was not able to reverse this effect (Fig. 3C).

4.3 Effect of prenatal hyperandrogenization on hepatic glucose metabolism

In order to analyze hepatic glucose metabolism, we analyze whether prenatal hyperandrogenization alters the gene expression of the main enzyme that catalyzes an irreversible step of gluconeogenesis; *pepck* and that of the glucose transporter *glut2*. We found that the gene expression of hepatic *pepck* is decreased in PHiov phenotype with a tendency to decrease in the PHanov phenotype (Fig. 4A, $p<0.001$) while metformin was able to reverse those alterations in both PH phenotypes. We also found that prenatal hyperandrogenization decreased ($p<0.01$) the gene expression of hepatic *Glut2* from both PH phenotypes and that metformin reversed this effect in the PHanov phenotype (Fig. 4B, $p<0.05$).

4.4 Effect of prenatal hyperandrogenization on liver energetic mediators

Regarding the transcription factors that are mediators of glycolysis, gluconeogenesis, glycogenolysis and lipogenesis, we found that the gene expression of *Chrebp* was lower in both PH phenotypes (PHiov, $p<0.05$, PHanov $p<0.01$) than in controls (Fig. 5A). Metformin treatment was able to reverse this decrease only in the PHanov phenotype ($p<0.05$) leading the *Chrebp* expression to control values (Fig. 5A).

Prenatal hyperandrogenization also decreased ($p<0.01$) the gene expression of *Srebp* in both phenotypes and metformin was not able to reverse this effect (Fig. 5B).

Prenatal hyperandrogenization also decreased the gene expression of hepatic *PPARg* ($p<0.05$) in both phenotypes (Fig. 5C), metformin was able to reverse this effect (Fig. 4C).

4.5 Effect of prenatal hyperandrogenization on energy storage and hepatic metabolism

To establish whether prenatal hyperandrogenization was able to alter hepatic energy storage, we evaluated hepatic reserves such as glycogen and TG, and found that neither of them was altered (Fig. 6A and 6B, respectively, $p>0.05$).

We also evaluated the serum levels of enzyme markers of hepatic function as: ALT, AST and GGT, and found that none of them were altered in either phenotype, and that metformin treatment was not able to reverse these alterations (Fig. 6C, 6D and 6E respectively, $p>0.05$).

The oxidant-antioxidant balance in liver tissue was evaluated by measuring lipid peroxidation index (LPO) and the content of the antioxidant glutathione (GSH). We found that prenatal hyperandrogenization increased LPO only in the PHanov phenotype (Fig. 7A, $p<0.05$) and that metformin reversed this effect (Fig 7A, $p<0.05$). GSH was

higher in the PHanov phenotype than in the control group (Fig 7B, $p<0.05$) and metformin reversed this effect (Fig 7B, $p<0.05$).

4.6 Effect of prenatal hyperandrogenization on circulating lipid profile

In order to determine the effect of prenatal hyperandrogenization on circulating lipid profile, we determined circulating levels of total cholesterol (Fig. 8A), HDL-cholesterol (Fig. 8B), LDL-cholesterol (Fig. 8C), and triglycerides (Fig. 8D). We found that prenatal hyperandrogenization increased LDL-cholesterol (Fig. 8C, $p<0.05$), and triglycerides (Fig. 8D, $p<0.05$), from both PH phenotypes. Metformin treatment only was able to reverse the adverse effect of prenatal hyperandrogenization on LDL-cholesterol. (Fig 8C).

4.7 Mechanism of metformin in the treatment of prenatal hyperandrogenization

It is known that metformin's primary mechanism of action is through AMPK activation, then, in order to determine its activation, we evaluated the protein expression of the substrate of activated AMPK, the phosphorylated acetyl CoA carboxylase (pACC). Figure 9 shows a representative Western Blot analysis of hepatic pACC protein expression. We found that metformin increased ($p<0.05$) the protein expression of pACC in both PH phenotypes.

5. Discussion

The present work aimed to study whether fetal programming by *in utero* androgen excess exposure is able to alter hepatic functions and whether metformin is able to reverse those possible alterations.

The position of a fetus, in relation to the sexes of its neighboring intrauterine littermates, can influence its exposure to gonadal hormones and, therefore, its development (Zielinski et al., 1991). This complex network of mechanisms involves not only plasticity phenomena (Bateson et al., 2014) but also differential placental dysfunctions. Moreover, a plastic phenotype has also been described in PCOS patients and their relatives (Jahanfar et al., 1995). Here, by means of an *in utero* programming rat model, we showed two well- differentiated phenotypes from the same mother: the PHiov and PHanov phenotypes.

It has been reported that prenatal androgen excess, and not the accumulation of adipose tissue, is the one that induces a state of insulin resistance (Dunaif et al., 1989; Jeanes and Reeves, 2017; Kahn and Flier, 2000; Saltiel and Kahn, 2001; Tewari et al., 2015). In agreement with this, we found an insulin resistance state without the presence of overweight or obesity.

Since metformin increases insulin sensitivity, it decreases insulin resistance and plasma fasting insulin levels (Diamanti-Kandarakis et al., 2010; Viollet et al., 2012). In this study, we found that metformin reversed the circulating insulin resistance state evaluated by HOMA-IR in both PH phenotypes, but partially reversed serum insulin levels, thus showing persistent hyperinsulinemia, which might in turn impair insulin signaling in peripheral tissues.

IR, IRS-1 and 2 are key mediators of many responses in insulin-sensitive tissues (White, 2002). Besides, hepatic *IRS2* gene expression is essential for insulin action (Valverde et al., 2003) and the failure of IRS2 signaling can lead to the eventual loss of the compensatory hyperinsulinemia during prolonged periods of insulin resistance (White, 2002). In addition, prenatal hyperandrogenism is one of the most important effects of fetal programming in inducing insulin resistance (Linden et al., 2018). In that context, we found that both PH phenotypes displayed hepatic insulin signaling disruption, as characterized by a decreased mRNA expression of *IR*, *IRS1* and *IRS2*, and that metformin reversed only the decrease in mRNA expression of *IRS1* in both phenotypes but not that of *IR* or *IRS2*. In agreement with these findings, the persistent hyperinsulinemia found after metformin treatment in both PH phenotypes could be explained by the failure of metformin to restore *IRS2* levels.

The enzyme PEPCK has been extensively studied for its importance in gluconeogenesis (Chakravarty et al., 2005; Hanson and Patel, 2006). The deletion of the gene for PEPCK

in the mouse liver alters gluconeogenesis (Hakimi et al., 2005; She et al., 2003) and results in profound hypoglycemia and death. However, other authors have found that increased expression of hepatic PEPCK is not associated with fasting hyperglycemia (Samuel et al., 2009). Testosterone down-regulates liver PEPCK, causing repression of the gluconeogenic pathway, which is impaired in a type 2 diabetes murine model (Pal and Gupta, 2016). Our data show that prenatal hyperandrogenization decreased the hepatic gene expression of PEPCK in both PH phenotypes and that metformin reversed the adverse effect of prenatal hyperandrogenization, increasing the hepatic gene expression of PEPCK to control values. This finding is not apparently in agreement with those of authors, who found that metformin inhibits PEPCK expression and hepatic gluconeogenesis (Foretz et al., 2010; Kim et al., 2008). However, we must consider that these authors reported enhanced expression of PEPCK before metformin treatment, whereas we found that the gene expression of PEPCK was decreased and that metformin led these decreased levels to control values. Further experiments are being designed to elucidate this point.

In the liver, glucose transport is carried out by GLUT2 (Nordlie et al., 1999) and hepatic *Glut2* gene expression is regulated by glucose metabolism (Rencurel et al., 1996). Therefore, *IRS2* knockout mice display alterations in liver glucose uptake (White, 2002). In agreement with these data, here we found a decrease in the gene expression of *IRS2* and *Glut2* in both PH phenotypes. Surprisingly, metformin was able to reverse the decrease in *Glut2* gene expression only in the PHanov phenotype. However, other glucose transporters less indispensable in the liver tissue, which may also be modulated by metformin, (Kinaan et al., 2015; Sokolovska et al., 2010) should be studied.

Hepatic SREBP and ChREBP, which are differentially regulated by insulin and glucose respectively (Iizuka and Horikawa, 2008; Wang et al., 2015), regulate genes that encode

enzymes for glucose metabolism or lipogenesis. Then, we suggest that the down-expression of both *Srebp* and *Chrebp* found in this study is a consequence of hepatic insulin signaling disruption. Metformin was able to reverse the decrease in *Chrebp* mRNA levels only in the PHanov phenotype, which is consistent with the up-regulation of *Glut2* by metformin. Moreover, given the established role of ChREBP in regulating glycolysis, we suggest that this may be a pathway of metformin action in regulating the bioavailability of glucose. Although metformin regulates *Chrebp* gene expression in other systems (Al-Oanzi et al., 2017; Berger et al., 2015; Iizuka, 2017; Kim et al., 2017), our data indicate, for the first time, that metformin is able to reverse the decrease in *Chrebp* gene expression induced by *in utero* androgen excess.

The other transcription factor studied was PPARG, which plays an important role in improving glucose homeostasis (Kallwitz et al., 2008), promoting lipid storage (Ables, 2012), and modulating SREBP (Kim and Spiegelman, 1996). In agreement with these data, we found that mRNA levels of *Pparg* were decreased in both PH phenotypes. This result is associated with the impaired glucose metabolism and decreased *Srebp* gene expression also found. Metformin was able to reverse these abnormalities, leading *Pparg* gene expression to control values, thus confirming that, as in other systems (El-Gharabawy et al., 2017; Mansour et al., 2017), metformin modulates hepatic glucose metabolism via the PPARG pathway.

Regarding the main enzymes involved in liver function, i.e., ALT, AST, and GGT, none of them was altered by the *in utero* androgen excess. Considering that these transaminases have been reported as markers of liver damage (Abruzzese et al., 2016; Vassilatou, 2014; Vassilatou et al., 2010), our findings suggest no signs of hepatic injury.

Triglycerides represent the main form of storage and transport of fatty acids in both hepatocytes and plasma (Alves-Bezerra and Cohen, 2017). Fatty acids accumulate in the liver by hepatocellular uptakes from the plasma and by *de novo* synthesis (Alves-Bezerra and Cohen, 2017). Triglycerides are frequently synthesized in states of energy excess, such as overnutrition and obesity (Choi and Diehl, 2008). In agreement with these findings, here we found no increase in body weight and consequently no alterations in hepatic glycogen or triglyceride content after *in utero* androgen excess. These data might explain the lower gene expression of the transcription factors involved in lipogenesis such as *Chrebp, Srebp*, and *Pparg* in both PH phenotypes.

One of the causes of insulin resistance is oxidative stress (ITO et al., 2006) and the state of non-compensated oxidative stress is involved in the hepatic damage (Abruzzese et al., 2016; Pan et al., 2004). Besides, insulin resistance increases fatty acid β-oxidation, leading to hepatic oxidative stress (Sanyal et al., 2001). In this sense, the administration of GSH, which is the most important low-molecular-weight antioxidant synthesized in cells, seems to be a promising strategy to treat oxidative stress-induced liver damage (Sacco et al., 2016). In this study, we found a pro-oxidant state characterized by increased lipid peroxidation and, as a compensatory mechanism, by an increase in the anti-oxidant GSH in the PHanov phenotype. These data suggest that prolonged oxidative stress may contribute to insulin resistance in the PHanov phenotype.

Because of its anti-hyperglycemic properties, metformin is a well-known therapy for type 2 diabetes. This drug acts on the AMPK pathway, which is a central metabolic regulator; however, there is increasing evidence that metformin also acts via AMPK-independent mechanisms (Pernicova and Korbonits, 2014). Studies have demonstrated that one of the primary effects of metformin is the decreased production of free radicals and reactive oxygen species through inhibition of mitochondrial complex I (Diniz Vilela

et al., 2016; Pernicova and Korbonits, 2014). In the present study, metformin treatment reversed the pro-oxidant state in the PHanov phenotype, thus suggesting that metformin action as an antioxidant may have contributed to ameliorating the derangements observed in the glucose and insulin pathways in the PHanov phenotype.

Hyperinsulinemia and hyperandrogenism lead to an altered lipid profile in both obese (Gholinezhad et al., 2018) and lean (Daghestani et al., 2018) women with PCOS. Here, we demonstrated that prenatal hyperandrogenization alters the circulating lipid profile, as previously reported in PCOS patients (Solymár et al., 2018; Xu et al., 2015), and that metformin activates AMPK and consequently reduces LDL-cholesterol. Metformin acts by inhibiting complex I in the electron transport chain (El-Mir et al., 2000; Owen et al., 2000) and mitochondrial suppression by metformin activates the AMPK cascade (Hawley et al., 2002; Zhou et al., 2001). In agreement with these findings, we found that metformin acts by increasing the protein expression of the acetyl CoA carboxylase (pACC), which is the substrate of activated AMPK.

Finally, our results showed that metformin treatment preferentially ameliorated the negative effect of the *in utero* androgen excess in the liver of the PHanov phenotype. Reproductive functions demand high energetic cost and good energy storage (Torre et al., 2014). Thus, the preferential action of metformin in the PHanov phenotype could account for the need to guarantee a good metabolic state to support the cost of reproduction. However, several studies are being carried out in our lab to clarify this point. In summary, the present work shows that metformin is able to reverse, in a phenotype precise manner, specific hepatic functions induced by *in utero* androgen excess exposure.

Funding

This work was supported by Agencia Nacional de Promoción Científica y Tecnológica (ANPCyT) (Grant PICT 577/2012 and PICT 689/2013), and Fundación Roemmers.

Acknowledgements

We thank Enzo Cuba and Marcela Marquez for their technical assistance in the animal care.

References

Ables, G.P. (2012). Update on Pparγ and Nonalcoholic Fatty Liver Disease. PPAR Res. *2012*.

Abruzzese, G.A., Heber, M.F., Ferreira, S.R., Velez, L.M., Reynoso, R., Pignataro, O.P., and Motta, A.B. (2016). Prenatal hyperandrogenism induces alterations that affect liver lipid metabolism. J. Endocrinol. *230*, 67–79.

Al-Oanzi, Z.H., Fountana, S., Moonira, T., Tudhope, S.J., Petrie, J.L., Alshawi, A., Patman, G., Arden, C., Reeves, H.L., and Agius, L. (2017). Opposite effects of a glucokinase activator and metformin on glucose-regulated gene expression in hepatocytes. Diabetes Obes. Metab. *19*, 1078–1087.

Alves-Bezerra, M., and Cohen, D.E. (2017). Triglyceride Metabolism in the Liver. Compr. Physiol. *8*, 1–8.

Amalfi, S., Velez, L.M., Heber, M.F., Vighi, S., Ferreira, S.R., Orozco, A.V., Pignataro, O., and Motta, A.B. (2012). Prenatal Hyperandrogenization Induces Metabolic and Endocrine Alterations Which Depend on the Levels of Testosterone Exposure. PLOS ONE *7*, e37658.

Barbieri, R.L., and Hornstein, M.D. (1988). Hyperinsulinemia and ovarian hyperandrogenism. Cause and effect. Endocrinol. Metab. Clin. North Am. *17*, 685–703.

Bateson, P., Gluckman, P., and Hanson, M. (2014). The biology of developmental plasticity and the Predictive Adaptive Response hypothesis. J. Physiol. *592*, 2357–2368.

Berger, E., Vega, N., Weiss-Gayet, M., and Géloën, A. (2015). Gene Network Analysis of Glucose Linked Signaling Pathways and Their Role in Human Hepatocellular Carcinoma Cell Growth and Survival in HuH7 and HepG2 Cell Lines. BioMed Res. Int. *2015*, 821761.

Book, C.B., and Dunaif, A. (1999). Selective insulin resistance in the polycystic ovary syndrome. J. Clin. Endocrinol. Metab. *84*, 3110–3116.

Bradford, M.M. (1976). A rapid and sensitive method for the quantitation of microgram quantities of protein utilizing the principle of protein-dye binding. Anal. Biochem. *72*, 248–254.

Caldwell, A.S.L., Middleton, L.J., Jimenez, M., Desai, R., McMahon, A.C., Allan, C.M., Handelsman, D.J., and Walters, K.A. (2014). Characterization of reproductive, metabolic, and endocrine features of polycystic ovary syndrome in female hyperandrogenic mouse models. Endocrinology *155*, 3146–3159.

Chakravarty, K., Cassuto, H., Reshef, L., and Hanson, R.W. (2005). Factors that control the tissue-specific transcription of the gene for phosphoenolpyruvate carboxykinase-C. Crit. Rev. Biochem. Mol. Biol. *40*, 129–154.

Choi, S.S., and Diehl, A.M. (2008). Hepatic triglyceride synthesis and nonalcoholic fatty liver disease. Curr. Opin. Lipidol. *19*, 295–300.

Chow, J.D.Y., Jones, M.E.E., Prelle, K., Simpson, E.R., and Boon, W.C. (2011). A selective estrogen receptor α agonist ameliorates hepatic steatosis in the male aromatase knockout mouse. J. Endocrinol. *210*, 323–334.

Corbould, A., and Dunaif, A. (2007). The adipose cell lineage is not intrinsically insulin resistant in polycystic ovary syndrome. Metabolism. *56*, 716–722.

Daghestani, M.H., Daghestani, M., Daghistani, M., El-Mazny, A., Bjørklund, G., Chirumbolo, S., Al Saggaf, S.H., and Warsy, A. (2018). A study of ghrelin and leptin levels and their relationship to metabolic profiles in obese and lean Saudi women with polycystic ovary syndrome (PCOS). Lipids Health Dis. *17*, 195.

De Fea, K., and Roth, R.A. (1997). Modulation of insulin receptor substrate-1 tyrosine phosphorylation and function by mitogen-activated protein kinase. J. Biol. Chem. *272*, 31400–31406.

Demissie, M., Lazic, M., Foecking, E.M., Aird, F., Dunaif, A., and Levine, J.E. (2008). Transient prenatal androgen exposure produces metabolic syndrome in adult female rats. Am. J. Physiol. Endocrinol. Metab. *295*, E262-268.

Diamanti-Kandarakis, E., Christakou, C.D., Kandaraki, E., and Economou, F.N. (2010). Metformin: an old medication of new fashion: evolving new molecular mechanisms and clinical implications in polycystic ovary syndrome. Eur. J. Endocrinol. *162*, 193–212.

Diniz Vilela, D., Gomes Peixoto, L., Teixeira, R.R., Belele Baptista, N., Carvalho Caixeta, D., Vieira de Souza, A., Machado, H.L., Pereira, M.N., Sabino-Silva, R., and Espindola, F.S. (2016). The Role of Metformin in Controlling Oxidative Stress in Muscle of Diabetic Rats.

Dunaif, A., Segal, K.R., Futterweit, W., and Dobrjansky, A. (1989). Profound peripheral insulin resistance, independent of obesity, in polycystic ovary syndrome. Diabetes *38*, 1165–1174.

El-Gharabawy, R.M., Ahmed, A.S., and Al-Najjar, A.H. (2017). Mechanism of action and effect of immune-modulating agents in the treatment of psoriasis. Biomed. Pharmacother. Biomedecine Pharmacother. *85*, 141–147.

Elia, E., Sander, V., Luchetti, C.G., Solano, M.E., Di Girolamo, G., Gonzalez, C., and Motta, A.B. (2006). The mechanisms involved in the action of metformin in regulating ovarian function in hyperandrogenized mice. Mol. Hum. Reprod. *12*, 475–481.

Elia, E.M., Belgorosky, D., Faut, M., Vighi, S., Pustovrh, C., Luigi, D., and Motta, A.B. (2009). The effects of metformin on uterine tissue of hyperandrogenized BALB/c mice. Mol. Hum. Reprod. *15*, 421–432.

El-Mir, M.-Y., Nogueira, V., Fontaine, E., Avéret, N., Rigoulet, M., and Leverve, X. (2000). Dimethylbiguanide Inhibits Cell Respiration via an Indirect Effect Targeted on the Respiratory Chain Complex I. J. Biol. Chem. *275*, 223–228.

Foretz, M., Hébrard, S., Leclerc, J., Zarrinpashneh, E., Soty, M., Mithieux, G., Sakamoto, K., Andreelli, F., and Viollet, B. (2010). Metformin inhibits hepatic gluconeogenesis in mice independently of the LKB1/AMPK pathway via a decrease in hepatic energy state. J. Clin. Invest. *120*, 2355–2369.

Fornes, R., Maliqueo, M., Hu, M., Hadi, L., Jimenez-Andrade, J.M., Ebefors, K., Nyström, J., Labrie, F., Jansson, T., Benrick, A., et al. (2017). The effect of androgen excess on maternal metabolism, placental function and fetal growth in obese dams. Sci. Rep. *7*, 8066.

Friedewald, W.T., Levy, R.I., and Fredrickson, D.S. (1972). Estimation of the concentration of low-density lipoprotein cholesterol in plasma, without use of the preparative ultracentrifuge. Clin. Chem. *18*, 499–502.

Gholinezhad, M., Gholsorkhtabaramiri, M., Esmaeilzadeh, S., and Ghanbarpour, A. (2018). Insulin resistance and adverse metabolic profile in overweight/obese and normal weight of young women with polycystic ovary syndrome. Casp. J. Intern. Med. *9*, 260–267.

Hakimi, P., Johnson, M.T., Yang, J., Lepage, D.F., Conlon, R.A., Kalhan, S.C., Reshef, L., Tilghman, S.M., and Hanson, R.W. (2005). Phosphoenolpyruvate carboxykinase and the critical role of cataplerosis in the control of hepatic metabolism. Nutr. Metab. *2*, 33.

Hanson, R.W., and Patel, Y.M. (2006). Phosphoenolpyruvate Carboxykinase (GTP): the Gene and the Enzyme. In Advances in Enzymology and Related Areas of Molecular Biology, (John Wiley & Sons, Ltd), pp. 203–281.

Hawley, S.A., Gadalla, A.E., Olsen, G.S., and Hardie, D.G. (2002). The Antidiabetic Drug Metformin Activates the AMP-Activated Protein Kinase Cascade via an Adenine Nucleotide-Independent Mechanism. Diabetes *51*, 2420–2425.

Heber, M.F., Ferreira, S.R., Vélez, L.M., and Motta, A.B. (2013). Prenatal hyperandrogenism and lipid profile during different age stages: an experimental study. Fertil. Steril. *99*, 551–557.

Heber, M.F., Ferreira, S.R., Abruzzese, G.A., Raices, T., Pignataro, O.P., Vega, M., and Motta, A.B. (2019). Metformin improves ovarian insulin signaling alterations caused by fetal programming. J. Endocrinol.

Iizuka, K. (2017). The transcription factor carbohydrate-response element-binding protein (ChREBP): A possible link between metabolic disease and cancer. Biochim. Biophys. Acta *1863*, 474–485.

Iizuka, K., and Horikawa, Y. (2008). ChREBP: a glucose-activated transcription factor involved in the development of metabolic syndrome. Endocr. J. *55*, 617–624.

ITO, Y., OUMI, S., NAGASAWA, T., and NISHIZAWA, N. (2006). Oxidative Stress Induces Phosphoenolpyruvate Carboxykinase Expression in H4IIE Cells. Biosci. Biotechnol. Biochem. *70*, 2191–2198.

Jahanfar, S., Eden, J.A., Warren, P., Seppälä, M., and Nguyen, T.V. (1995). A twin study of polycystic ovary syndrome**Supported by The Academy of Finland, the

University of Helsinki, the Nordisk Forsknings Kommitte and the Cancer Society of Finland (M.S.). Fertil. Steril. *63*, 478–486.

Jeanes, Y.M., and Reeves, S. (2017). Metabolic consequences of obesity and insulin resistance in polycystic ovary syndrome: diagnostic and methodological challenges. Nutr. Res. Rev. *30*, 97–105.

Kahn, B.B., and Flier, J.S. (2000). Obesity and insulin resistance. J. Clin. Invest. *106*, 473–481.

Kallwitz, E.R., McLachlan, A., and Cotler, S.J. (2008). Role of peroxisome proliferators-activated receptors in the pathogenesis and treatment of nonalcoholic fatty liver disease. World J. Gastroenterol. *14*, 22–28.

Kim, J.B., and Spiegelman, B.M. (1996). ADD1/SREBP1 promotes adipocyte differentiation and gene expression linked to fatty acid metabolism. Genes Dev. *10*, 1096–1107.

Kim, Y.D., Park, K.-G., Lee, Y.-S., Park, Y.-Y., Kim, D.-K., Nedumaran, B., Jang, W.G., Cho, W.-J., Ha, J., Lee, I.-K., et al. (2008). Metformin inhibits hepatic gluconeogenesis through AMP-activated protein kinase-dependent regulation of the orphan nuclear receptor SHP. Diabetes *57*, 306–314.

Kim, Y.S., Kim, M., Choi, M.Y., Lee, D.H., Roh, G.S., Kim, H.J., Kang, S.S., Cho, G.J., Kim, S.-J., Yoo, J.-M., et al. (2017). Metformin protects against retinal cell death in diabetic mice. Biochem. Biophys. Res. Commun. *492*, 397–403.

Kinaan, M., Ding, H., and Triggle, C.R. (2015). Metformin: An Old Drug for the Treatment of Diabetes but a New Drug for the Protection of the Endothelium. Med. Princ. Pract. *24*, 401–415.

Lashen, H. (2010). Role of metformin in the management of polycystic ovary syndrome. Ther. Adv. Endocrinol. Metab. *1*, 117–128.

Lee, M., Katerelos, M., Gleich, K., Galic, S., Kemp, B.E., Mount, P.F., and Power, D.A. (2018). Phosphorylation of Acetyl-CoA Carboxylase by AMPK Reduces Renal Fibrosis and Is Essential for the Anti-Fibrotic Effect of Metformin. J. Am. Soc. Nephrol. JASN *29*, 2326–2336.

Legro, R.S., Kunselman, A.R., Dodson, W.C., and Dunaif, A. (1999). Prevalence and predictors of risk for type 2 diabetes mellitus and impaired glucose tolerance in polycystic ovary syndrome: a prospective, controlled study in 254 affected women. J. Clin. Endocrinol. Metab. *84*, 165–169.

Linden, A.G., Li, S., Choi, H.Y., Fang, F., Fukasawa, M., Uyeda, K., Hammer, R.E., Horton, J.D., Engelking, L.J., and Liang, G. (2018). Interplay between ChREBP and SREBP-1c coordinates postprandial glycolysis and lipogenesis in livers of mice. J. Lipid Res. *59*, 475–487.

Mansour, H.H., El Kiki, S.M., and Galal, S.M. (2017). Metformin and low dose radiation modulates cisplatin-induced oxidative injury in rat via PPAR-γ and MAPK pathways. Arch. Biochem. Biophys. *616*, 13–19.

Matthews, D.R., Hosker, J.P., Rudenski, A.S., Naylor, B.A., Treacher, D.F., and Turner, R.C. (1985). Homeostasis model assessment: insulin resistance and β-cell function from fasting plasma glucose and insulin concentrations in man. Diabetologia *28*, 412–419.

Nordlie, R.C., Foster, J.D., and Lange, A.J. (1999). Regulation of glucose production by the liver. Annu. Rev. Nutr. *19*, 379–406.

Owen, M.R., Doran, E., and Halestrap, A.P. (2000). Evidence that metformin exerts its anti-diabetic effects through inhibition of complex 1 of the mitochondrial respiratory chain. Biochem. J. *348*, 607–614.

Pal, M., and Gupta, S. (2016). Testosterone supplementation improves glucose homeostasis despite increasing hepatic insulin resistance in male mouse model of type 2 diabetes mellitus. Nutr. Diabetes *6*, e236.

Pan, M., Cederbaum, A.I., Zhang, Y.-L., Ginsberg, H.N., Williams, K.J., and Fisher, E.A. (2004). Lipid peroxidation and oxidant stress regulate hepatic apolipoprotein B degradation and VLDL production. J. Clin. Invest. *113*, 1277–1287.

Pernicova, I., and Korbonits, M. (2014). Metformin--mode of action and clinical implications for diabetes and cancer. Nat. Rev. Endocrinol. *10*, 143–156.

Previs, S.F., Withers, D.J., Ren, J.M., White, M.F., and Shulman, G.I. (2000). Contrasting effects of IRS-1 versus IRS-2 gene disruption on carbohydrate and lipid metabolism in vivo. J. Biol. Chem. *275*, 38990–38994.

Rencurel, F., Waeber, G., Antoine, B., Rocchiccioli, F., Maulard, P., Girard, J., and Leturque, A. (1996). Requirement of glucose metabolism for regulation of glucose transporter type 2 (GLUT2) gene expression in liver. Biochem. J. *314 (Pt 3)*, 903–909.

Sacco, R., Eggenhoffner, R., and Giacomelli, L. (2016). Glutathione in the treatment of liver diseases: insights from clinical practice. Minerva Gastroenterol. Dietol. *62*, 316–324.

Saltiel, A.R., and Kahn, C.R. (2001). Insulin signalling and the regulation of glucose and lipid metabolism. Nature *414*, 799–806.

Samuel, V.T., Beddow, S.A., Iwasaki, T., Zhang, X.-M., Chu, X., Still, C.D., Gerhard, G.S., and Shulman, G.I. (2009). Fasting hyperglycemia is not associated with increased expression of PEPCK or G6Pc in patients with Type 2 Diabetes. Proc. Natl. Acad. Sci. *106*, 12121–12126.

Sanyal, A.J., Campbell–Sargent, C., Mirshahi, F., Rizzo, W.B., Contos, M.J., Sterling, R.K., Luketic, V.A., Shiffman, M.L., and Clore, J.N. (2001). Nonalcoholic steatohepatitis: Association of insulin resistance and mitochondrial abnormalities. Gastroenterology *120*, 1183–1192.

Seifter, S., and Dayton, S. (1950). The estimation of glycogen with the anthrone reagent. Arch. Biochem. *25*, 191–200.

She, P., Burgess, S.C., Shiota, M., Flakoll, P., Donahue, E.P., Malloy, C.R., Sherry, A.D., and Magnuson, M.A. (2003). Mechanisms by which liver-specific PEPCK knockout mice preserve euglycemia during starvation. Diabetes *52*, 1649–1654.

Sokolovska, J., Isajevs, S., Sugoka, O., Sharipova, J., Lauberte, L., Svirina, D., Rostoka, E., Sjakste, T., Kalvinsh, I., and Sjakste, N. (2010). Influence of metformin on GLUT1 gene and protein expression in rat streptozotocin diabetes mellitus model. Arch. Physiol. Biochem. *116*, 137–145.

Solymár, M., Ivic, I., Pótó, L., Hegyi, P., Garami, A., Hartmann, P., Pétervári, E., Czopf, L., Hussain, A., Gyöngyi, Z., et al. (2018). Metformin induces significant reduction of body weight, total cholesterol and LDL levels in the elderly – A meta-analysis. PLOS ONE *13*, e0207947.

Sun, M., Maliqueo, M., Benrick, A., Johansson, J., Shao, R., Hou, L., Jansson, T., Wu, X., and Stener-Victorin, E. (2012). Maternal androgen excess reduces placental and fetal weights, increases placental steroidogenesis, and leads to long-term health effects in their female offspring. Am. J. Physiol. Endocrinol. Metab. *303*, E1373-1385.

Swillens, S., Dessars, B., and Housni, H.E. (2008). Revisiting the sigmoidal curve fitting applied to quantitative real-time PCR data. Anal. Biochem. *373*, 370–376.

Tewari, N., Awad, S., Macdonald, I.A., and Lobo, D.N. (2015). Obesity-related insulin resistance: implications for the surgical patient. Int. J. Obes. 2005 *39*, 1575–1588.

Torre, S.D., Benedusi, V., Fontana, R., and Maggi, A. (2014). Energy metabolism and fertility—a balance preserved for female health. Nat. Rev. Endocrinol. *10*, 13–23.

Valverde, A.M., Burks, D.J., Fabregat, I., Fisher, T.L., Carretero, J., White, M.F., and Benito, M. (2003). Molecular mechanisms of insulin resistance in IRS-2-deficient hepatocytes. Diabetes *52*, 2239–2248.

Vassilatou, E. (2014). Nonalcoholic fatty liver disease and polycystic ovary syndrome. World J. Gastroenterol. *20*, 8351–8363.

Vassilatou, E., Lafoyianni, S., Vryonidou, A., Ioannidis, D., Kosma, L., Katsoulis, K., Papavassiliou, E., and Tzavara, I. (2010). Increased androgen bioavailability is associated with non-alcoholic fatty liver disease in women with polycystic ovary syndrome. Hum. Reprod. Oxf. Engl. *25*, 212–220.

Viollet, B., Guigas, B., Sanz Garcia, N., Leclerc, J., Foretz, M., and Andreelli, F. (2012). Cellular and molecular mechanisms of metformin: an overview. Clin. Sci. Lond. Engl. 1979 *122*, 253–270.

Wang, Y., Viscarra, J., Kim, S.-J., and Sul, H.S. (2015). Transcriptional regulation of hepatic lipogenesis. Nat. Rev. Mol. Cell Biol. *16*, 678–689.

White, M.F. (2002). IRS proteins and the common path to diabetes. Am. J. Physiol.-Endocrinol. Metab. *283*, E413–E422.

Wolf, C.J., Hotchkiss, A., Ostby, J.S., LeBlanc, G.A., and Gray, L.E. (2002). Effects of Prenatal Testosterone Propionate on the Sexual Development of Male and Female Rats: A Dose-Response Study. Toxicol. Sci. *65*, 71–86.

Xu, T., Brandmaier, S., Messias, A.C., Herder, C., Draisma, H.H.M., Demirkan, A., Yu, Z., Ried, J.S., Haller, T., Heier, M., et al. (2015). Effects of metformin on metabolite profiles and LDL cholesterol in patients with type 2 diabetes. Diabetes Care *38*, 1858–1867.

Zhou, G., Myers, R., Li, Y., Chen, Y., Shen, X., Fenyk-Melody, J., Wu, M., Ventre, J., Doebber, T., Fujii, N., et al. (2001). Role of AMP-activated protein kinase in mechanism of metformin action. J. Clin. Invest. *108*, 1167–1174.

Zielinski, W.J., Vandenbergh, J.G., and Montano, M.M. (1991). Effects of social stress and intrauterine position on sexual phenotype in wild-type house mice (Mus musculus). Physiol. Behav. *49*, 117–123.

Legends of figures

Figure 1. Schematic diagram of murine model and metformin treatment.
The diagram displays the murine model of prenatal hyperandrogenization. PH= prenatally hyperandrogenized group, PHiov= irregular ovulatory prenatally hyperandrogenized group, PHanov= anovulatory prenatally hyperandrogenized group, met = metformin.

Figure 2. Effect of prenatal hyperandrogenism on circulating insulin resistance. Metabolic features evaluated in female offspring of control and prenatally hyperandrogenized (PH) groups with and without metformin treatment. (A) Basal glucose levels, (B) Basal insulin levels, (C) HOMA-IR index. Each column represent the mean ± SD (N= 10 replicates per group), a vs b $p < 0.05$ by Two-way ANOVA test.

Figure 3. Effect of prenatal hyperandrogenization on disrupting of hepatic insulin signaling
The graphs correspond to the mRNA abundance of the gene of interest relative to *L32* mRNA levels of control and prenatally hyperandrogenized (PH) groups with and without metformin treatment. (A) Insulin receptor (IR), (B) Insulin receptor substrate 1 (IRS1), (C) Insulin receptor substrate 2 (IRS2). Each column represent the mean ± SD (N= 6 replicates per group), a vs b $p < 0.05$ by Two-way ANOVA test.

Figure 4. Effect of prenatal hyperandrogenization on the hepatic glucose metabolism. The graphs correspond to the mRNA abundance of the gene of interest relative to *L32* mRNA levels of control and prenatally hyperandrogenized (PH) groups with and without metformin treatment of (A) *pepck-1* and (B) *glut2*. Each column represent the mean ± SD (N= 6 replicates per group), a vs b $p < 0.05$ by Two-way ANOVA test.

Figure 5. Effect of prenatal hyperandrogenization on liver energetic mediators.

The graphs correspond to the mRNA abundance of the gene of interest relative to *L32* mRNA levels of control and prenatally hyperandrogenized (PH) groups with and without metformin treatment. (A) *Chrebp*, (B) *Shrebp*, (C) *Pparg*. Each column represent the mean ± SD (N= 6 replicates per group), a vs b $p < 0.05$ by Two-way ANOVA test.

Figure 6. Effect of prenatal hyperandrogenization on energy storage and hepatic metabolism. (A) Glycogen content, (B) Tygliceride content, (C) liver transaminase ALT, (D) liver transaminase AST, (E) liver transaminase GGT corresponding to control and prenatally hyperandrogenized (PH) groups with and without metformin treatment. Each column represent the mean ± SD (N= 10 replicates per group) by Two-way ANOVA test.

Figure 7. Effect of prenatal hyperandrogenization on hepatic oxidative stress. The oxidant/antioxidant balance in liver tissue was evaluated by measuring the lipid peroxidation LPO (A) and the content of the antioxidant glutathione (B) corresponding to control and prenatally hyperandrogenized (PH) groups with and without metformin treatment. Each column represent the mean ± SD (N= 10 replicates per group), a vs b $p < 0.05$ by Two-way ANOVA test.

Figure 8. Effect of prenatal hyperandrogenization on circulating lipid profile. Serum levels of (A) total cholesterol, (B) high-density lipoprotein (HDL) cholesterol, (C) low-density lipoprotein (LDL) cholesterol, and (D) triglycerides (TG) corresponding to control and prenatally hyperandrogenized (PH) groups with and without metformin treatment. Each column represent the mean ± SD (N= 7 replicates per group), a vs b $p < 0.05$ by Two-way ANOVA test.

Figure 9. Mechanism of metformin in the treatment of prenatal hyperandrogenization

A representative Western Blot analysis of phosphorylated acetyl CoA carboxylase (pACC) corresponding to control and prenatally hyperandrogenized (PH) groups with and without metformin treatment. Each column represent the mean ± SD (N= 7 replicates per group) by Two-way ANOVA test.

Table 1 List of primers used in real-time PCR.

Gene	Forward primer (5´-3´)	Reverse primer (5´-3´)
IR	ATG GGA CCA CTG TAC GCT TC	TCG ATC CGT TCT CGA AGA CT
IRS-1	TGT GCC AAG CAA CAA GAA AG	ACG GTT TCA GAG CAG AGG AA
IRS-2	GGA AGT CTG TTC GGG TGT GT	ACA TCT GCT TCA GTG TGC TG
GLUT2	GTT TTG GGT GTT CCT CTG GA	TGA TCC TTC CGA GTT TGT CC
PPARG	TTT TCA AGG GTG CCA GTT TC	GAG GCC AGC ATG GTG TAG AT
SREBP	TAACCTGGCTGAGTGTGCAG	ATCCACGAAGAAACGGTGAC
CHREBP	GGTTGTCCCCAAAGCAGAGA	TTGTTGTCTACACGACCCCG
PEPCK	GGAGACCACAGGATGAGGAA	TTCGTAGACAAGGGGGACAC
PSMB2	TCG GAG TCG GAC CCC TTA TC	TGT AGT AAA GTG CTG GCC CC
RPL32	TGG TCC ACA ATG TCA AGG	CAA AAC AGG CAC ACA AGC

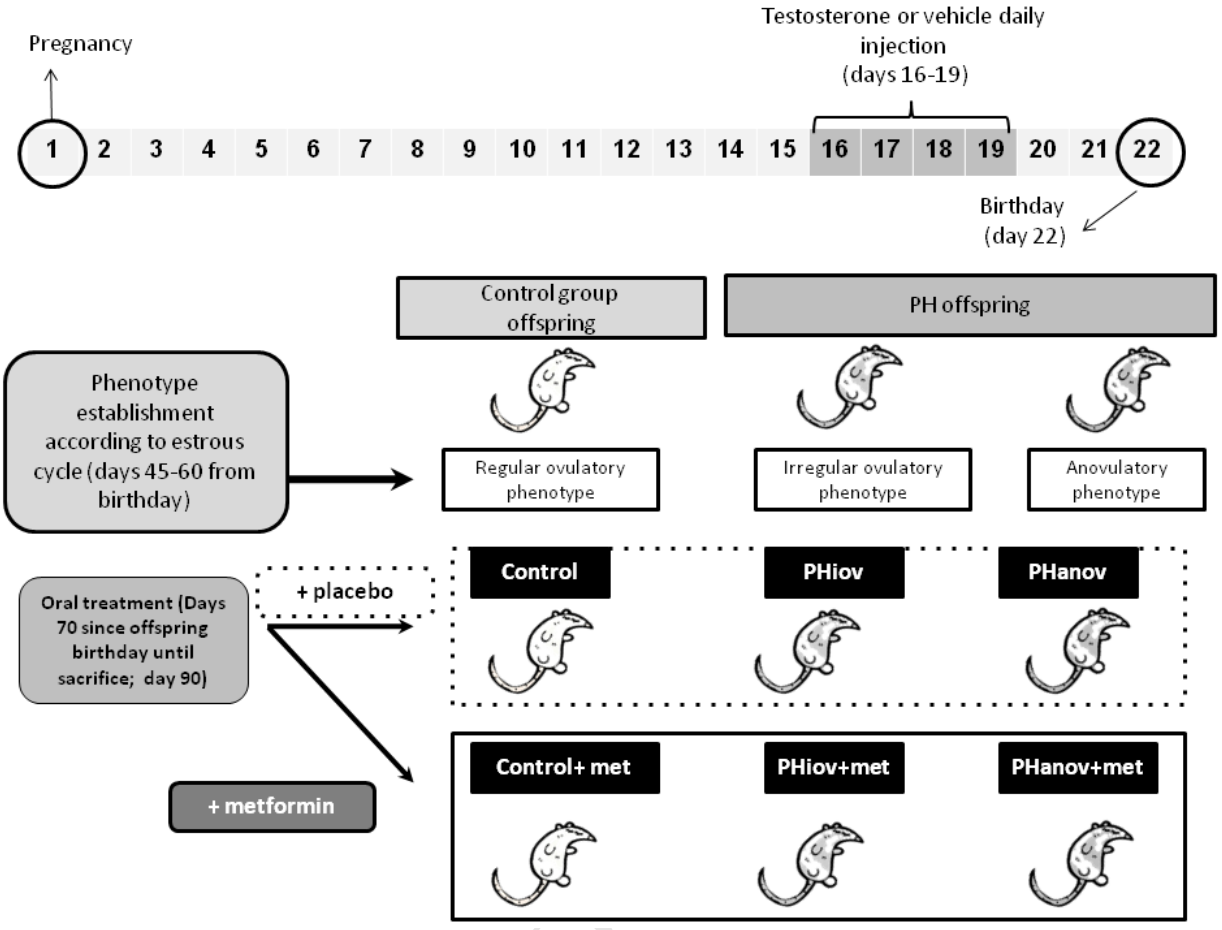
Pregnancy
Testosterone or vehicle daily injection (days 16-19)
1 2 3 4 5 6 7 8 9 10 11 12 13 14 15 16 17 18 19 20 21 22
Birthday (day 22)
Control group offspring
PH offspring
Phenotype establishment according to estrous cycle (days 45-60 from birthday)
Regular ovulatory phenotype
Irregular ovulatory phenotype
Anovulatory phenotype
Oral treatment (Days 70 since offspring birthday until sacrifice; day 90)
+ placebo
+ metformin
Control
PHiov
PHanov
Control+ met
PHiov+met
PHanov+met

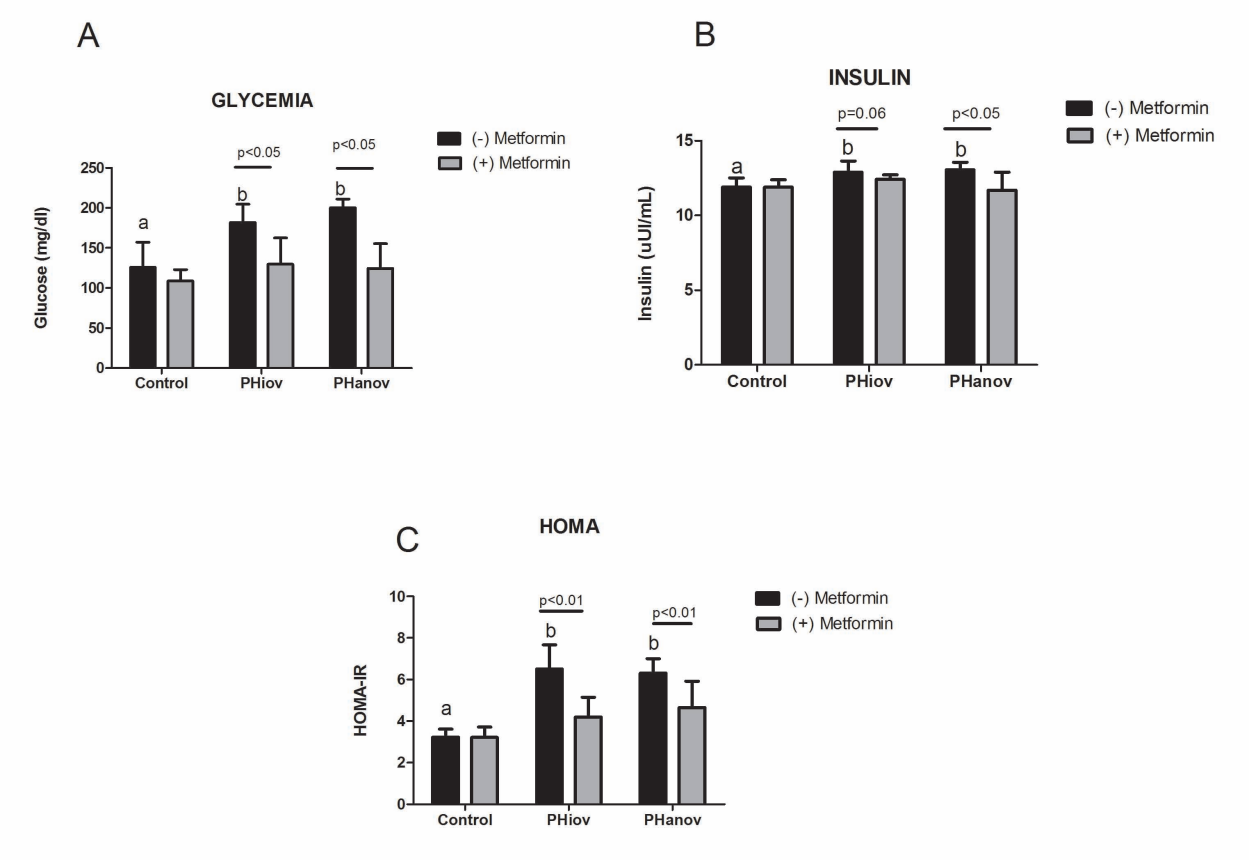

A

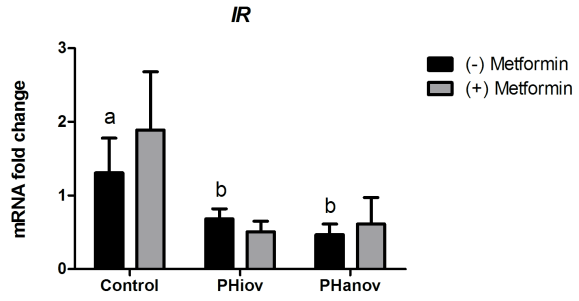

B

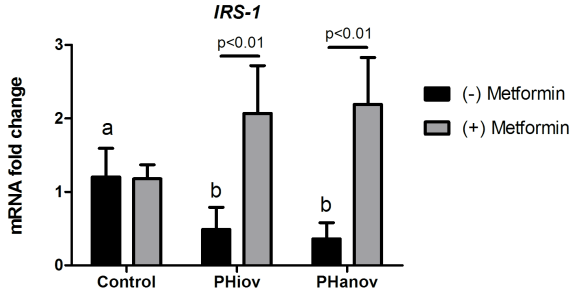

C

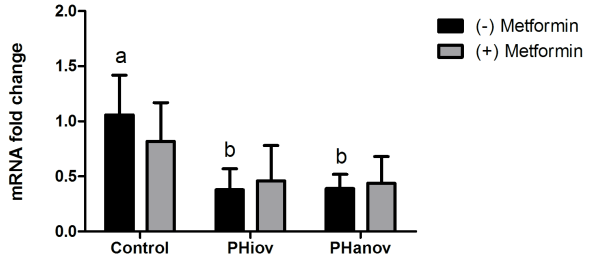

A

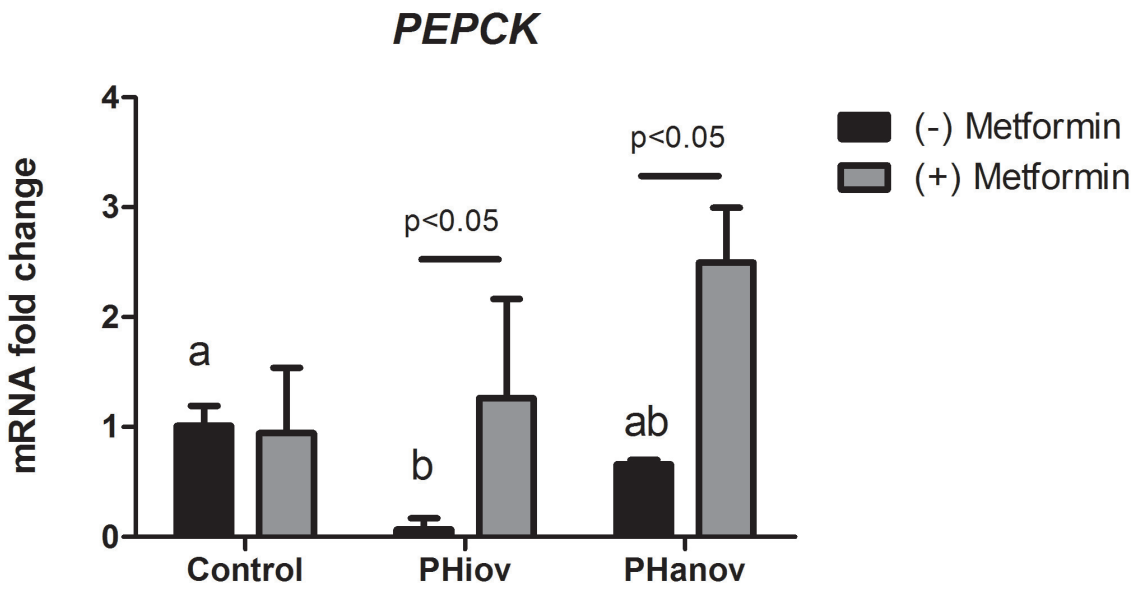
PEPCK
mRNA fold change
4
3
2
1
0
a
b
ab
p<0.05
p<0.05
Control
PHiov
PHanov
(-) Metformin
(+) Metformin

B

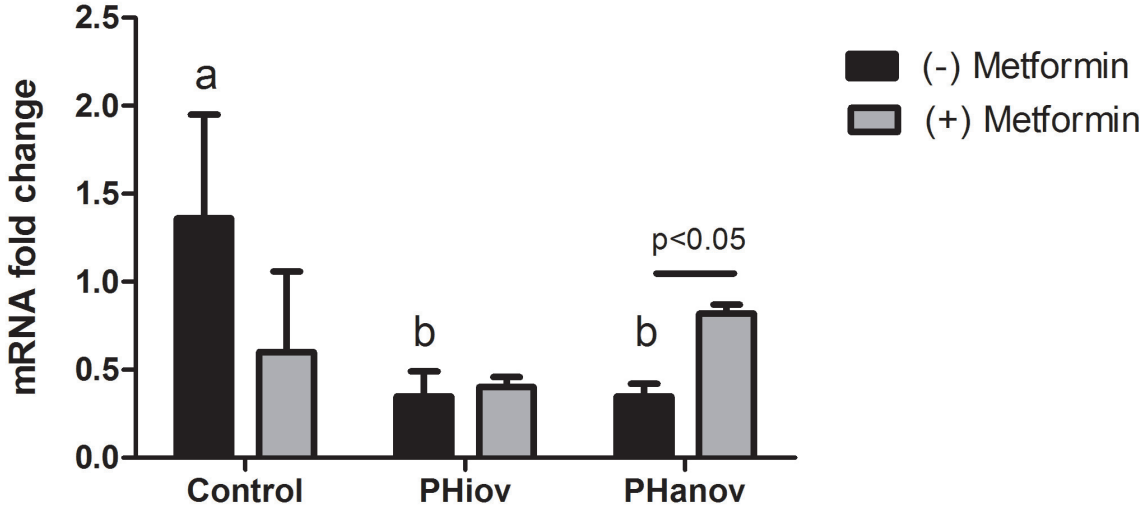
GLUT2
mRNA fold change
2.5
2.0
1.5
1.0
0.5
0.0
a
b
b
p<0.05
Control
PHiov
PHanov
(-) Metformin
(+) Metformin

A

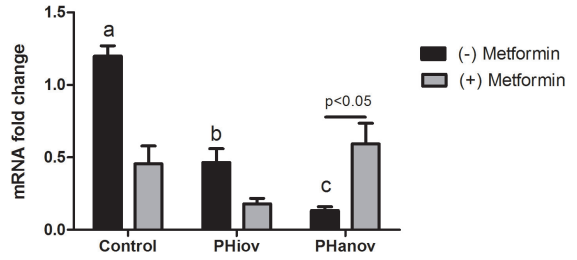

B

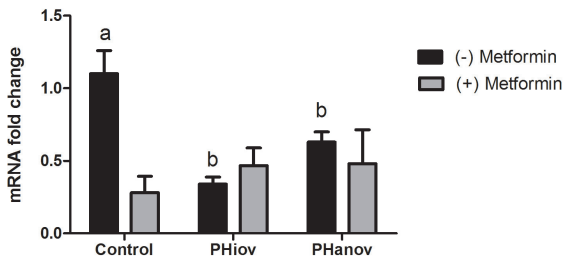

C

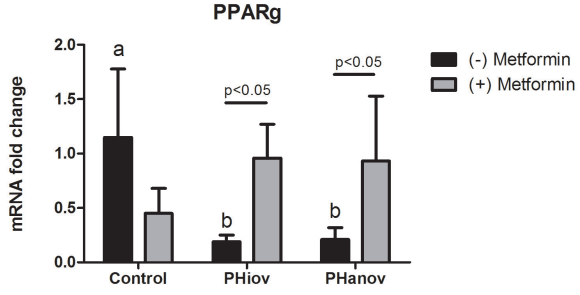

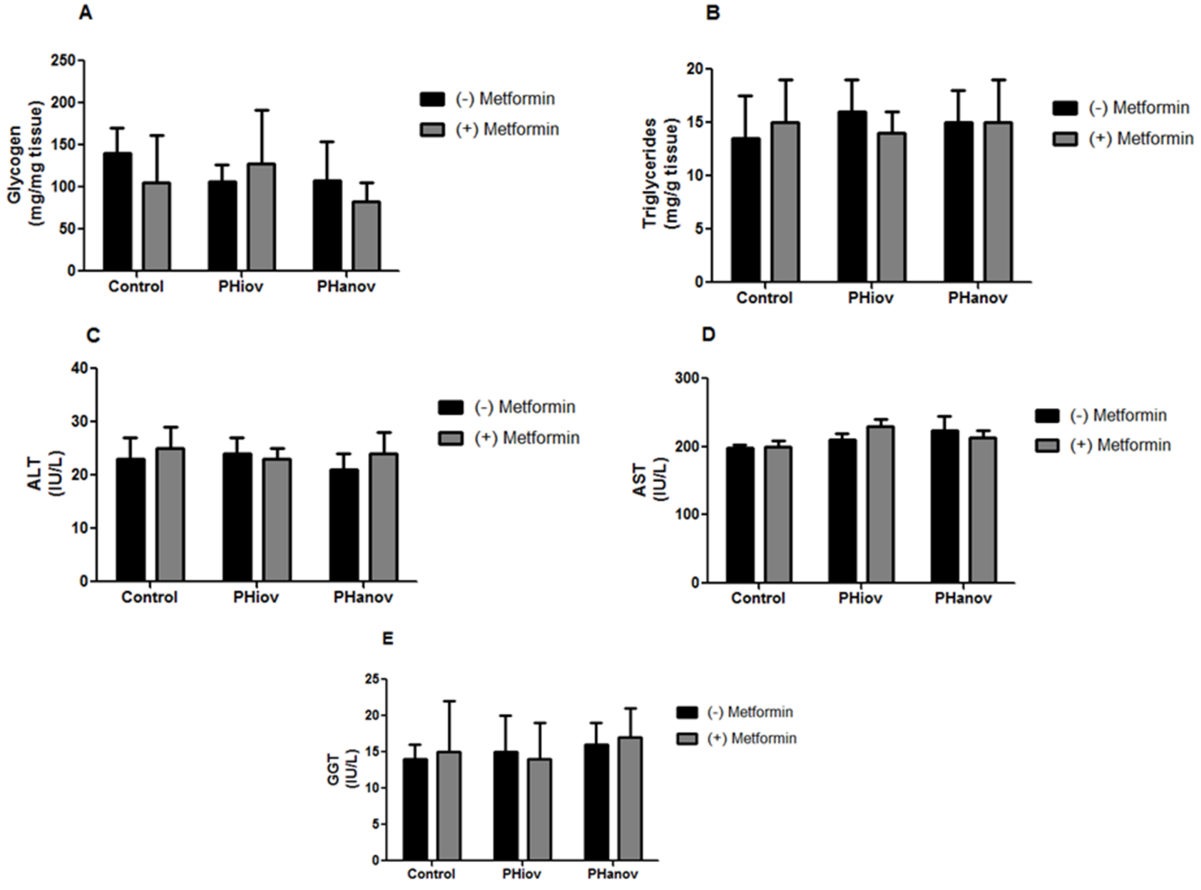
A
Glycogen (mg/mg tissue)
250
200
150
100
50
0
Control
PHiov
PHanov
(-) Metformin
(+) Metformin
B
Triglycerides (mg/g tissue)
20
15
10
5
0
Control
PHiov
PHanov
(-) Metformin
(+) Metformin
C
ALT (IU/L)
40
30
20
10
0
Control
PHiov
PHanov
(-) Metformin
(+) Metformin
D
AST (IU/L)
300
200
100
0
Control
PHiov
PHanov
(-) Metformin
(+) Metformin
E
GGT (IU/L)
25
20
15
10
5
0
Control
PHiov
PHanov
(-) Metformin
(+) Metformin

A

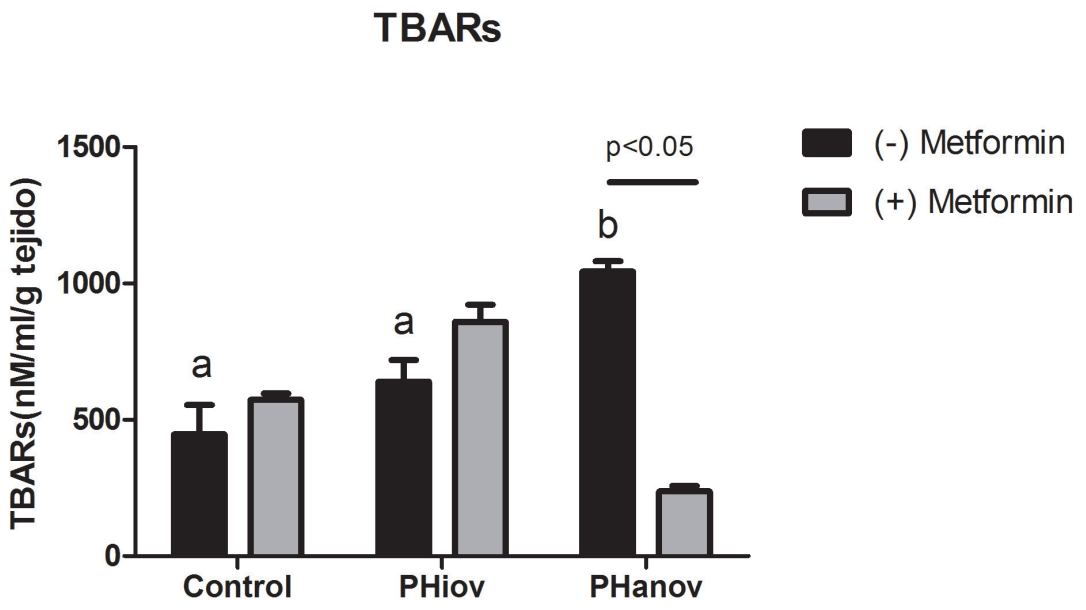
TBARs
TBARs(nM/ml/g tejido)
1500
1000
500
0
p<0.05
a
a
b
Control
PHiov
PHanov
(-) Metformin
(+) Metformin

B

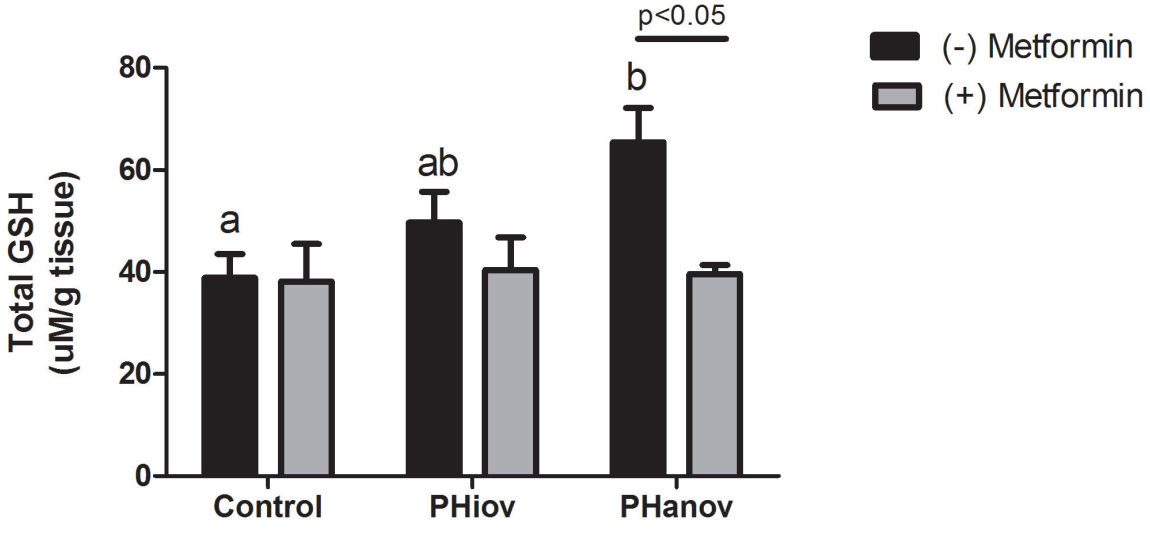
Total GSH
Total GSH (uM/g tissue)
80
60
40
20
0
p<0.05
a
ab
b
Control
PHiov
PHanov
(-) Metformin
(+) Metformin

A

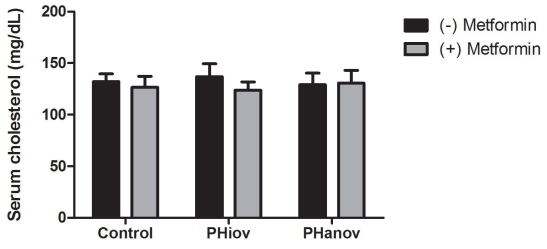

B

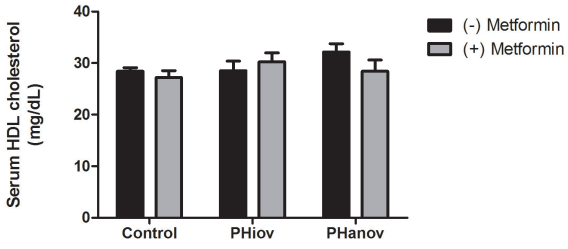

C

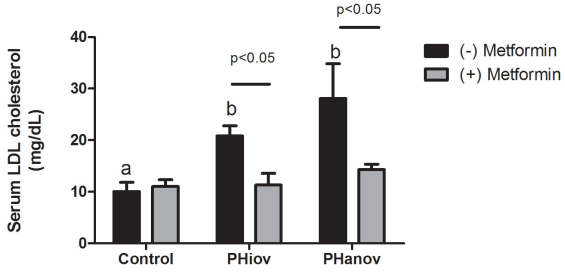

D

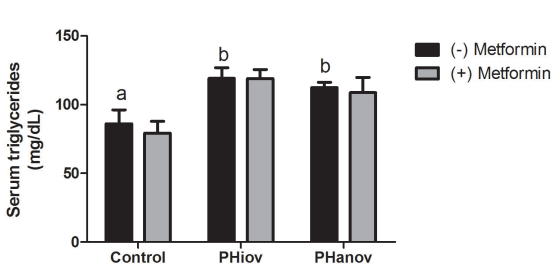

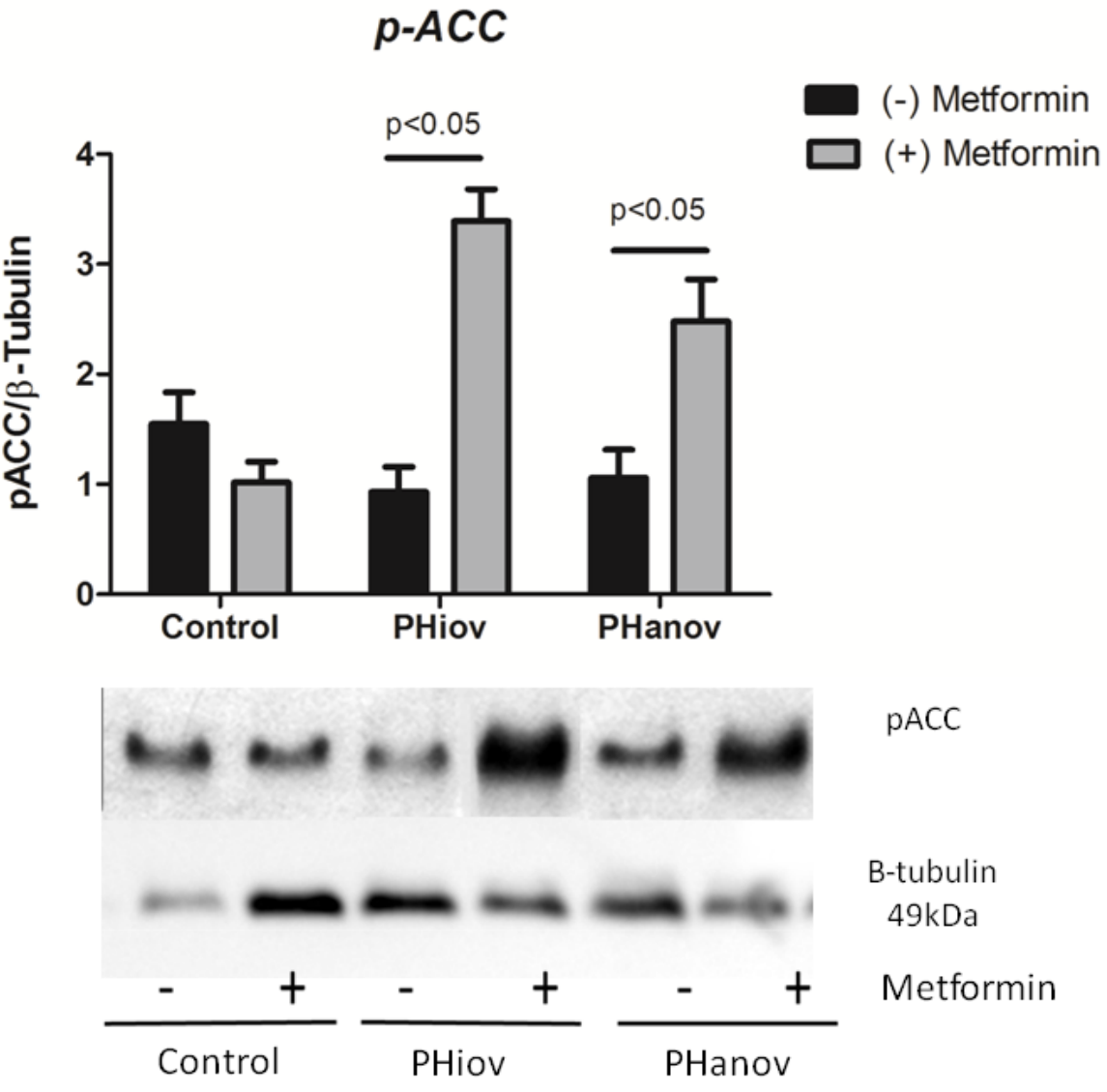
p-ACC
(-) Metformin
(+) Metformin
p<0.05
p<0.05
pACC/β-Tubulin
4
3
2
1
0
Control
PHiov
PHanov
pACC
B-tubulin
49kDa
- + - + - +
Metformin
Control
PHiov
PHanov

Credit Author Statement

Giselle Adriana Abruzzese: treatment of animals, preparation of the experiments, statistical analysis of results, revision of the manuscript

María Florencia Heber: treatment of animals, preparation of the experiments, statistical analysis of results, revision of the manuscript

María José Ferrer: preparation of the experiments, analysis of results, revision of the manuscript

Silvana Rocío Ferreira: treatment of animals, preparation of the experiments, statistical analysis of results, revision of the manuscript

Aimé Silva: preparation of the experiments, revision of the manuscript

Alicia B Motta: statistical analysis of results, analysis of results, writing of the manuscript